Redox Biology 41 (2021) 101940

Contents lists available at ScienceDirect

Redox Biology

journal homepage: www.elsevier.com/locate/redox

Methionine restriction alleviates age-associated cognitive decline via fibroblast growth factor 21

Bo Ren [a,1], Luanfeng Wang [a,1], Lin Shi [b], Xin Jin [c], Yan Liu [a], Rui Hai Liu [d], Fei Yin [e], Enrique Cadenas [f], Xiaoshuang Dai [c], Zhigang Liu [a,d,*], Xuebo Liu [a,**]

[a] Laboratory of Functional Chemistry and Nutrition of Food, College of Food Science and Engineering, Northwest A&F University, Yangling, Shaanxi, 712100, China
[b] College of Food Engineering and Nutritional Science, Shaanxi Normal University, Shaanxi, 710119, China
[c] BGI Institute of Applied Agriculture, BGI-Shenzhen, Shenzhen, 518120, China
[d] Department of Food Science, Cornell University, Ithaca, 14853-7201, NY, USA
[e] Center for Innovation in Brain Science and Department of Pharmacology, University of Arizona, Tucson, 85721, AZ, USA
[f] Pharmacology and Pharmaceutical Sciences, School of Pharmacy, University of Southern California, Los Angeles, 90089, CA, USA

ARTICLE INFO

Keywords:
Methionine restriction
Aging
Cognitive decline
Fibroblast growth factor 21
Nrf2
Oxidative stress

ABSTRACT

Methionine restriction (MR) extends lifespan and delays the onset of aging-associated pathologies. However, the effect of MR on age-related cognitive decline remains unclear. Here, we find that a 3-month MR ameliorates working memory, short-term memory, and spatial memory in 15-month-old and 18-month-old mice by preserving synaptic ultrastructure, increasing mitochondrial biogenesis, and reducing the brain MDA level in aged mice hippocampi. Transcriptome data suggest that the receptor of fibroblast growth factor 21 (FGF21)-related gene expressions were altered in the hippocampi of MR-treated aged mice. MR increased FGF21 expression in serum, liver, and brain. Integrative modelling reveals strong correlations among behavioral performance, MR altered nervous structure-related genes, and circulating FGF21 levels. Recombinant FGF21 treatment balanced the cellular redox status, prevented mitochondrial structure damages, and upregulated antioxidant enzymes HO-1 and NQO1 expression by transcriptional activation of Nrf2 in SH-SY5Y cells. Moreover, knockdown of *Fgf21* by *i.v.* injection of adeno-associated virus abolished the neuroprotective effects of MR in aged mice. In conclusion, the MR exhibited the protective effects against age-related behavioral disorders, which could be partly explained by activating circulating FGF21 and promoting mitochondrial biogenesis, and consequently suppressing the neuroinflammation and oxidative damages. These results demonstrate that FGF21 can be used as a potential nutritional factor in dietary restriction-based strategies for improving cognition associated with neurodegeneration disorders.

1. Introduction

The elderly population is increasing worldwide [1,2] and the incidence of age-related neurodegenerative disorders associated with cognitive decline is on the rise [3]. Multiple biological processes such as inflammation, neurobiological changes, diet, and lifestyle contribute to age-related cognitive decline [4]. Dietary patterns, including calorie and protein restrictions, have been widely reported to affect longevity or mitigate age-related diseases and metabolic syndrome [5–9]. Methionine restriction (MR), which reduces the essential amino acid methionine (Met) in diet, extends lifespan in yeast, *Drosophila*, and rodents [10–12]. MR reduces oxidative damage and changes the lipid composition in the brain [13,14], which may contribute to neuronal vitality. Furthermore, MR improved the impairment of working memory and spatial memory in high fat diet (HFD)-induced obese mice [15,16]. However, the protective effect of MR on age-related cognitive decline and its underlying mechanism remain unclear.

Fibroblast growth factor 21 (FGF21) is a member of the FGF family, which is primarily expressed in the liver and adipose tissue [17]. Several metabolic functions of MR have been shown to be mediated by FGF21

* Corresponding author. Laboratory of Functional Chemistry and Nutrition of Food, College of Food Science and Engineering, Northwest A&F University, Yangling, Shaanxi, 712100, China.
** Corresponding author.
E-mail addresses: zhigangliu@nwsuaf.edu.cn (Z. Liu), xueboliu@nwsuaf.edu.cn (X. Liu).
[1] These authors contributed equally.

https://doi.org/10.1016/j.redox.2021.101940
Received 19 January 2021; Received in revised form 5 March 2021; Accepted 6 March 2021
Available online 11 March 2021

[18–20]. FGF21 acts directly via its receptor FGFR1/β-klotho, which stimulates the secretion of lipolysis-related hormones and activates AMPK signaling to promote energy metabolism and extend lifespan [21]. Activation of nuclear factor erythroid 2–related factor 2 (Nrf2) signaling by FGF21 leads to the transcriptional activation of antioxidant genes [20]. FGF21 can potentially affect neural functions and FGF21 administration suppresses an oxidative stress response and inflammatory cytokine production in the brain of D-galactose-treated mice [22]. FGF21 receptors, including FGFR1 and β-klotho, are also expressed in the brain. Peripheral FGF21 can cross the blood-brain barrier and interact with β-klotho to promote remyelination in the central nervous system [23,24]. Recombinant human FGF21 (rFGF21) restores synaptic plasticity, dendritic spine density, and cerebral mitochondrial function and improves cognition in obese rats [25]. FGF21 attenuates HFD-induced cognitive impairment and anxiety-like behavior via metabolic modulation and anti-inflammatory responses in a mouse model [26]. Mitochondrial dysfunction is known to contribute to the development of neurodegenerative disorders. In human dopaminergic neurons, FGF21 enhances mitochondrial function and activates PGC-1α [27]. These findings support the hypothesis that FGF21 plays a vital role in promoting cognitive function under the dietary intervention of MR.

In this study, we aim at defining the protective effect of MR on age-related cognition decline and sought to investigate whether FGF21 in the brain is a critical mediator of neuronal functions. We find that MR improved cognition by activating circulating FGF21 and further protecting synaptic ultrastructure and enhancing mitochondrial biogenesis genes. These results may contribute to developing new dietary strategies against the cognitive decline inherent in aging and some neurodegenerative disorders, thus acquiring considerable clinical value.

2. Materials and methods

2.1. Short hairpin design and AAV production

The sequence of *Fgf21* (*Mus musculus*, NCBI Gene ID: 56636) was analyzed for suitable sequences for RNA interference-mediated silencing. A negative control (NC, 5′-TTCTCCGAACGTGTCACGT-3′) or shFGF21 (5′-GGGATTCAACACAGGAGAAAC-3′) with a TTCAAGAGA hairpin loop and TTTTTT termination sequence were generated, annealed, and cloned into a pAAV-U6-eGFP entry vector (Shanghai GenePharma Co., Ltd). After plaque selection and amplification, all viruses were purified using a discontinuous CsCl gradient. The final titer of AAV-shFGF21 was 1.6×10^{12}. The effect of AAV-shFGF21 *in vivo* was evaluated in aged C57BL/6J mice (see Supplementary Methods).

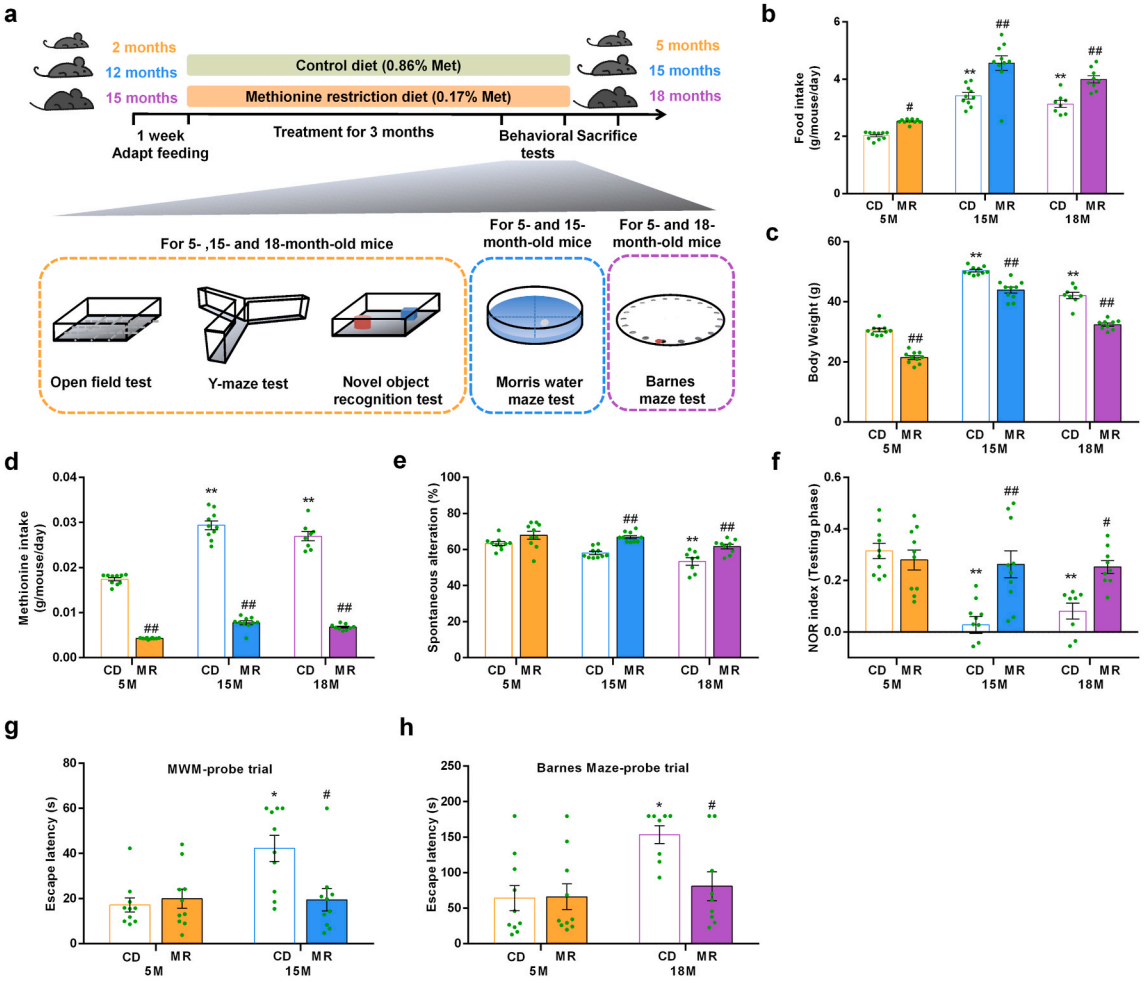

Fig. 1. Methionine restriction alleviated cognitive impairment in aged mice.
(a) Schedule of animal treatments and behavior tests (n = 8–10 mice per group); **(b)** Bodyweight; **(c)** Methionine intake. The cognitive functions were assessed using the behavioral tests as described in Methods; **(d)** Locomotor activity; **(e)** Spontaneous alteration; **(f)** NOR index (new object); **(g)** Escape latency (Morris water maze test); **(h)** Escape latency (Barnes maze test). Data show mean ± SEM. $^{*}p < 0.05$, $^{**}p < 0.01$ compared to the CD group. Significant differences between mean values were determined using two-way ANOVA with Tukey's multiple comparison test. Significant differences between mean values were determined using two-way ANOVA with Tukey's multiple comparison test.

2.2. Mouse experiments and dietary intervention

Male and female C57BL/6J mice of different ages were used in this study. All mice were originally obtained from Beijing Vital River Laboratory Animal Technology Co., Ltd., and housed in the Northwest A&F University animal facility under standard conditions at 22 ± 2 °C and 50 ± 15% humidity with a strict 12 h: 12 h light: dark cycle. The animals were fed *ad libitum* before the dietary prevention and AAV treatments.

For the first set of animals, male C57BL/6J mice (2-, 12-, and 15-month-old) were treated with a control methionine diet (0.86% Met) and methionine restriction diet (0.17% Met) for 3 months (n = 10) (Fig. 1a). The detailed dietary composition is provided in Supplementary Data. Two mice in the 18M-CD group and one mouse in the 18M-MR group died during the dietary intervention, data of which were excluded. Body weight, food intake, and water consumption were recorded, and methionine intake was calculated.

The second set of mice (2- and 15- month-old) were treated with AAV-shFGF21 (5×10^9 p.f.u. viruses per mouse, tail vein injection) and subjected to the same regimen of MR intervention (n = 8). AAV injections were administered twice, one before adaptive feeding and one in the middle of the experiment.

For the third set of animals, male and female C57BL/6J mice (15-month-old) were treated with control methionine diet and methionine restriction diet for 3 months (n = 8). The dietary intervention method, behavioral experiment schedule, and sample collection method were the same as those used for the first set of animals.

After the MR regimen, cognitive behavior was assessed using behavioral tests. After the behavioral tests, the mice were killed, and the serum and tissue samples were collected by snap-freezing in liquid nitrogen and storing at −80 °C or by directly storing in 4% paraformaldehyde for histological analysis.

All experimental procedures were performed according to the Guide for the Care and Use of Laboratory Animals: Eighth Edition (ISBN-10: 0-309-15396-4). All relevant ethical regulations for animal testing were followed, and the research protocols were approved by the Northwest A&F University and BGI Institutional Review Board on Bioethics and Biosafety (BGI-IRB).

2.3. Open field test

The open field test was used to assess locomotor activity. The open field apparatus consisted of a square box (length: 30 cm, width: 30 cm, height: 40 cm) and a locomotor monitoring system. The testing area was divided into a center area and four corner areas. Each mouse was placed in the center of the box and allowed 5 min of spontaneous activity. The SuperMaze software (Shanghai Xinruan Information Technology Co., Ltd, China) was used to record and measure the total distance traveled, total distance traveled in the central region, resting time, and time spent in the central region.

2.4. Y-maze test

The Y-maze was composed of three arms at 120° each. Each mouse was placed in the center of the Y-maze and allowed free exploration to all three arms for 8 min. The percentage alternation was calculated as the ratio of actual to possible alternations (defined as the total number of arm entries − 2) × 100%.

2.5. Novel object recognition test

The experimental process of the novel object recognition test consisted of three sessions: habituation, training, and test session. During the first session, each mouse was placed in the center of an open field box without objects for 5 min. The next day, each mouse was placed in the box for 10 min with two identical odorless objects that were placed equidistant from each other in this training session. On the third day, the same process was conducted for the test session; however, one object was replaced by a novel object. The apparatus was cleaned with 70% ethanol between each trial interval. The mice were considered to exhibit object exploration when they licked, sniffed, and touched the objects with the paws or head within a distance of 2 cm from the object. Furthermore, the percentage NOR index was used to discriminate the novel object in the test session:

$$\text{NOR index} = \left(\frac{\textit{novel object exploration time} - \textit{familiar object exploration time}}{\textit{total exploration time}} \right)$$

2.6. Morris water maze (MWM) test

The MWM test was used to examine the spatial learning ability and memory of the rodents per our previous study with some modifications [28]. Briefly, MWM testing was conducted in a circular pool filled with water with white food-grade titanium dioxide (XR-XM101, Shanghai Xinruan Information Technology Co. Ltd, Shanghai, China). The pool was divided into four conceptual quadrants of equal area. On day 0, each mouse received four habituation-training sessions. The platform was visible, and the water was colorless on day 0, whereas the opacity of water was increased to hide the submerged platform on day 1 to day 6. On day 6, the platform was removed from the maze and a probe trail was conducted in which mice were placed in the pool for 60 s. The video tracking system recorded the time spent in the target quadrant, the latency to the platform, and the number of platform crossings (SuperMaze software).

2.7. Barnes maze test

The Barnes maze is also a definitive test for examining the spatial learning and memory of mice. Each mouse was placed in the maze and allowed to explore for 5 min of adaptation trials. On the next day, the bright light was used to motivate mice to enter the hidden escape box during the 7-day training (two training trials per day). The maze has the same designated escape position for each mouse. However, the mouse was randomly assigned to one of the four different escape positions to overcome bias. Each mouse was placed under an opaque start box in the center of the maze for 30 s to explore the platform freely, after which the start box was lifted. The trial ended when the mouse had climbed into the hidden escape or after 5 min had elapsed. The maze and escape box were wiped with 70% ethanol after each trial and the maze was rotated. All data were recorded using a video tracking system (SuperMaze software).

2.8. Transmission electron microscopy (TEM)

The hippocampi of mice were collected, fixed with 2.5% glutaraldehyde (*v/v*) for 4 h, and then washed thrice with 0.1 M phosphate buffered saline (PBS), pH 7.2. Then, the tissue was fixed in 1% OsO_4 for 1 h. Next, the tissue was washed again with PBS and successively dehydrated with 30%, 50%, 70%, 80%, 90%, and 100% ethanol for 15 min each. Finally, the LR-WHITE was embedded and dried in an oven at 60 °C. The samples stained with uranyl acetate and lead citrate were acquired using a JEM-1230 transmission electron microscope (JEOL, Tokyo, Japan).

2.9. Real-time polymerase chain reaction (RT-PCR)

Total RNA from the brain and liver tissues was extracted using TRIzol (Jingcai Bio., Xi'an, China). The HiFiScript cDNA synthesis kit was used for reverse transcribing the RNA. RT-PCR was performed in a CFX96TM real-time system (Bio-Rad). The following cycling conditions were used: 95 °C for 10 min, then 95 °C for 15s, and 60°C for 1 min for 40 cycles. The $2^{-\Delta\Delta CT}$ method was used to analyze the relative changes in gene expression. For mitochondrial DNA (mtDNA, COX2) and nuclear DNA

(nDNA, globin), the total DNA was extracted from cortex tissue using a DNA extraction kit (Bioteke Co., Beijing, China). The primer sequences are shown in the Supplementary Table 2.

2.10. RNA-sequencing and data analysis

The reads were filtered and trimmed using Trimmomatic v0.38. Clean reads were mapped to the *Mus musculus* genome sequence (ftp://ftp.ncbi.nlm.nih.gov/genomes/all/GCF/000/001/635/GCF_000001635.26_GRCm38.p6) using Hisat2 v2-2.1.0. The reads of each sample were then assembled into transcripts and compared with reference gene models using StringTie v1.3.4d. We merged the 44 transcripts to obtain a consensus transcript using the StringTie-Merge program. Transcripts that did not exist in the CDS database of the *Mus musculus* genome were extracted to predict new genes. The gene expression FPKM values were calculated using StringTie based on the consensus transcript. A repeated double cross-validation framework (rdCV-PLSDA) and a multivariate dimension reduction method, DIABLO, were used for multiple RNA-seq data and clinical data, as described previously. GSEA was conducted using the GSEA v4.1.0 for Windows [29,30]. Curated gene sets (C2) from the Molecular Signatures Database (MSigDB) version 7.2 and Gene Ontology sets (C5) were evaluated using GSEA. Normalized enrichment scores (NESs) and adjusted q values were computed using the GSEA method based on 1,000 random permutations of the ranked genes.

2.11. Cell culture

SH-SY5Y cells were provided by the Kunming Institute of Zoology, Chinese Academy of Sciences (Kunming, China), and cultured in Dulbecco's minimal essential medium (DMEM) (Gibco Co., USA) supplemented with 10% fetal bovine serum (FBS), 100 IU mL^{-1} penicillin, and 100 μg mL^{-1} streptomycin at 37 °C in a humidified atmosphere of 5% CO_2. For Western blot assay, the cultured cells were treated with 100 nM rFGF21 for 12 h and extracted using a protein extraction reagent. To evaluate the effect of FGF21 on oxidative stress, the cultured cells were treated with 100 nM rFGF21 for 12 h, following which the medium was discarded and the cells were treated with or without H_2O_2 (100 μM) for 24 h. Intracellular redox status was determined by dyeing with 10 μM H_2DCFDA for 20–30 min at 37 °C in the dark. Fluorescence was observed using an inverted fluorescence microscope and quantified using a multimode microplate reader at 485 nm excitation and 538 nm emission. Mitochondrial dysfunction was detected by staining with 10 μM JC-1 for 30 min at 37 °C in the dark. Fluorescence was observed using an inverted fluorescence microscope and quantified using a multimode microplate reader at 485 nm excitation and 538 nm (green) and 585 nm (red) emissions.

2.12. Western blotting

Proteins were extracted using a protein extraction reagent. The total proteins were separated via sodium dodecyl sulfate-polyacrylamide gel electrophoresis and then transferred onto a polyvinylidene fluoride membrane using a wet transfer apparatus. Appropriate antibodies were used, and the immunoreactive bands were visualized using an enhanced chemiluminescence reagent. The information regarding primary antibodies is shown in Supplementary Table 1. The results of the Western blot were quantified using band densitometry analysis of the Quantity One software.

2.13. Statistical analysis

Other than RNA sequencing data, other data were reported as mean ± SEM, significant differences between mean values were determined by two-way ANOVA. A post hoc test was performed using Tukey's test for multiple comparison test by Graphpad Prism 6.0 software. Means were considered to be statistically significant if $p < 0.05$.

3. Results

3.1. MR suppresses age-dependent cognitive impairment

Two-month-old, 12-month-old, and 15-month-old C57BL/6J mice were fed either a control diet (CD; 0.86% Met, *w/w*) or a methionine restricted diet (MR; 0.17% Met, *w/w*) for three months (Fig. 1a). At the end of the dietary intervention, the food intake and body weight of the 15-month-old-CD and 18-month-old-CD mice (initial age was 12 months and 15 months, respectively) were significantly higher compared to 5-month-old-CD mice (initial age was 2 months); analysis of variance (two-way ANOVA with Tukey's test, $p < 0.01$). The body weights of mice fed the MR diet were lower than those of mice in the control group, despite an increased food intake (Fig. 1b and c). Met intake was significantly reduced in mice fed the MR diet (two-way ANOVA with Tukey's test, $p < 0.01$; Fig. 1d). It is noteworthy that the serum Met level increased in 15 month-old-CD mice, whereas MR intervention reduced Met levels to a level similar to that in the 5 month-old-CD group (Supplementary Data 1, Supplementary Fig. 1). In addition, fatty liver was observed in the 15- and 18-month-old-CD, and MR reduced lipid accumulation in liver (Supplementary Fig. 2).

Our previous studies have shown that 15-month-old C57BL/6J mice exhibited reduced working memory and spatial memory dysfunction [31,32]. The effects of MR on cognitive impairment in aged mice were assessed using several behavioral tests after dietary intervention. An open field test was conducted to evaluate the locomotive activity and exploring ability. The locomotor activity of mice in the three age groups did not differ significantly after the dietary intervention (Supplementary Fig. 3A). However, MR decreased the resting time and increased the time spent in the central area in aged mice (Supplementary Fig. 3B and C). The Y-maze test was performed to understand the effects of MR on working memory. The spontaneous alteration of 15- and 18-month-old-CD mice was significantly poorer than that of 5-month-old-CD mice (two-way ANOVA with Tukey's test, $p < 0.01$). Conversely, the spontaneous alteration was recovered in the MR-treated group (Fig. 1e). A novel object recognition test (NOR) was performed to understand the effects of MR on short-term memory. In the training phase, the mice explored in an open field with two identical objects. The NOR index did not differ significantly between age-matched CD and MR groups (Supplementary Fig. 3D). However, in the testing phase, one of the objects was replaced by a different object, and MR treatment restored the decrease in age-related NOR index of mice in the 15- and 18-month-old group (two-way ANOVA with Tukey's test, $p < 0.05$; Fig. 1f).

The Morris water maze (MWM) and Barnes maze were used to evaluate spatial memory [33,34]. Considering the excessive stress that swimming induces in aged mice, the water maze was conducted on 5- and 15-month-old mice, and the Barnes maze was conducted on 5- and 18-month-old mice. MWM and Barnes maze were conducted using the same schedule, including a place navigation test and probe trial test. In the MWM 3-day and 5-day place navigation test, MR improved the escape latency of 15-month-old mice (Fig. 1g, Supplementary Fig. 3G). In the probe trial test, MR enhanced the number of platform crossings in the targeting area and the percentage of distance in the targeting quadrant of 15-month-old mice (two-way ANOVA with Tukey's test, $p < 0.05$; Supplementary Fig. 3E and F). Similarly, in the 5-day Barnes maze place navigation test, MR improved the escape latency of 18-month-old mice (two-way ANOVA with Tukey's test, $p < 0.05$; Fig. 1h). In the probe trial test, the 5-month-old mice showed frequent movement close to the targeting box. MR increased the number of entries near the targeting box in 18-month-old mice (Supplementary Fig. 3J). The representative paths are shown in Supplementary Fig. 3H and I. These experiments demonstrate that MR ameliorates age-induced cognitive impairment.

3.2. MR improves synapse ultrastructure and mitochondrial biogenesis in the hippocampus

The hippocampus is the neural basis of cognitive function [35]. Representative micrographs of hematoxylin and eosin (H & E)-stained mouse hippocampus are shown in Supplementary Fig. 2. In particular, neuronal degeneration and nuclear shrinkage were observed in the dentate gyrus region of aged mice, while MR protected against neuronal damage (Supplementary Fig. 2). To investigate the effect of MR on synaptic function, the ultrastructure of the synapses and mitochondrial morphology in the hippocampi of 5-, 15-, and 18-month-old mice were assessed by transmission electron microscopy (TEM; Fig. 2a). Analysis of postsynaptic density (PSD) revealed that both the length and width of the PSD were elevated in the 15- and 18-month-old-MR groups (two-way ANOVA with Tukey's test, $p < 0.01$). While MR did not affect the length and width of PSD in 5-month-old mice (Fig. 2b and c). MR increased the length and width of the PSD in the 15- and 18-month-old-MR groups compared to those in the age-matched CD groups (two-way ANOVA with Tukey's test, $p < 0.01$). PSD95 is an essential structural protein required for postsynaptic density [36]. Quantitative polymerase chain reaction (qPCR) analysis confirmed that MR elevated the mRNA level of *Psd95* in 18-month-old mice (two-way ANOVA with Tukey's test, $p < 0.05$; Fig. 2d).

Fragmental phenotype and irregular shape of mitochondria were also observed in age-matched CD groups (colored asterisks in Fig. 2a), whereas MR decreased the ratio of abnormal mitochondria to normal mitochondria in 15- and 18-month-old mice (Fig. 2e). To investigate mitochondrial biogenesis in MR-fed aged mice, the mtDNA/nDNA ratio (represent by *Cox2/globin* ratio) in the cortex and the expression of *Pgc1α* in the hippocampus were determined. The *Cox2/globin* ratio and *Pgc1α* mRNA level did not change in 5- and 15 month-old mice on MR diet. In 18 month-old mice, the *Cox2/globin* ratio and *Pgc1α* mRNA levels were elevated by MR (two-way ANOVA with Tukey's test, $p < 0.05$; Fig. 2f and g). These results suggest that MR improves synapse ultrastructure and mitochondrial biogenesis in the hippocampi of aged mice.

3.3. MR affects nervous structure-related genes and FGF21 receptor expression in the hippocampus

To further investigate how MR regulates vital biological processes and pathways in the brain, we performed RNA-seq of mouse hippocampi (Supplementary Data 2). After mapping clean RNA-seq reads of all mice against the *Mus musculus* genome, we detected 13,218 genes (including 3,187 new predicted genes with no annotation) with fragments per kilobase of transcripts per million mapped reads (FPKM) value (Supplementary Data 3). Gene set enrichment analysis (GSEA) has been commonly used for pathway or functional analysis of RNA-seq data. The top 10 enrichments gene sets of GSEA in curated gene sets and ontology gene sets (based on Molecular Signatures Database), respectively, was listed according to normalized enrichment score (NES; Fig. 3a). The results show that one of the top-rank enriched gene set Reactome_Signaling_By_FGFR1 were downregulated in 18-month-old MR mice hippocampi (NES = −1.98, NOM p-val < 0.0001; Fig. 3c). Heatmap representations of gene expression differences between 18-month-old-CD and 18 month-old-MR mice revealed opposite expression patterns (Fig. 3b). The mRNA levels of *Fgfr1* and *β-klotho* were significantly increased with age but decreased by MR treatment (two-way ANOVA with Tukey's test, $p < 0.01$; Fig. 3d). Genes upregulated by MR were associated with biological pathways, including GO_Myelin_Sheath and GO_Ensheathment_Of_Neurons (Fig. 3a). FGF21 decreased with age in

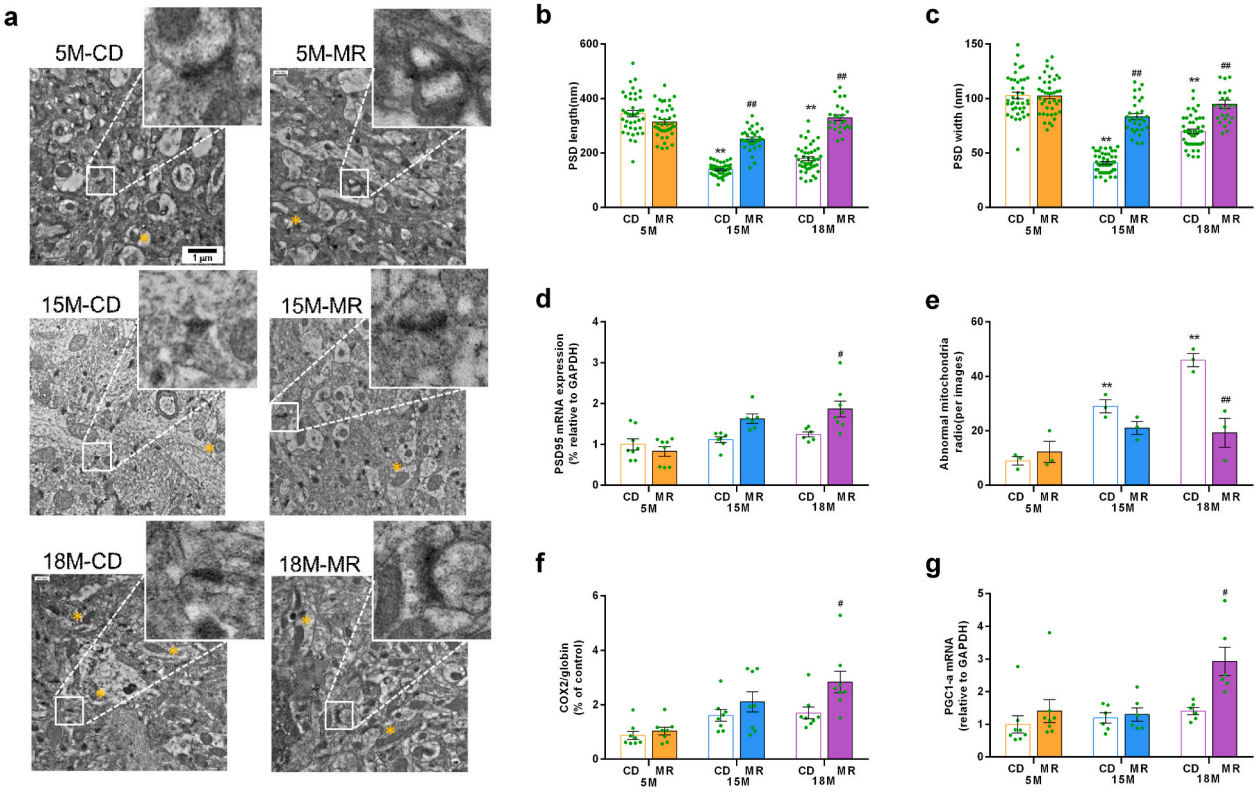

Fig. 2. Methionine restriction improved synapse ultrastructure and altered mitochondrial biogenesis in the aged mice hippocampus.
(a) Representative images showing the ultrastructure of the synapse. The yellow asterisks indicate the abnormal mitochondria; **(b, c)** The length and width of PSD (n = 3 slices per group); **(d)** *Psd95* mRNA expression detected using qRT-PCR; **(e)** Abnormal mitochondria ratio; **(f)** Mitochondrial DNA levels in brain tissue; **(g)** *Pgc1α* mRNA expression in the hippocampus. Data show mean ± SEM. *$p < 0.05$, **$p < 0.01$ compared to the CD group. Significant differences between mean values were determined using two-way ANOVA with Tukey's multiple comparison test. (For interpretation of the references to color in this figure legend, the reader is referred to the Web version of this article.)

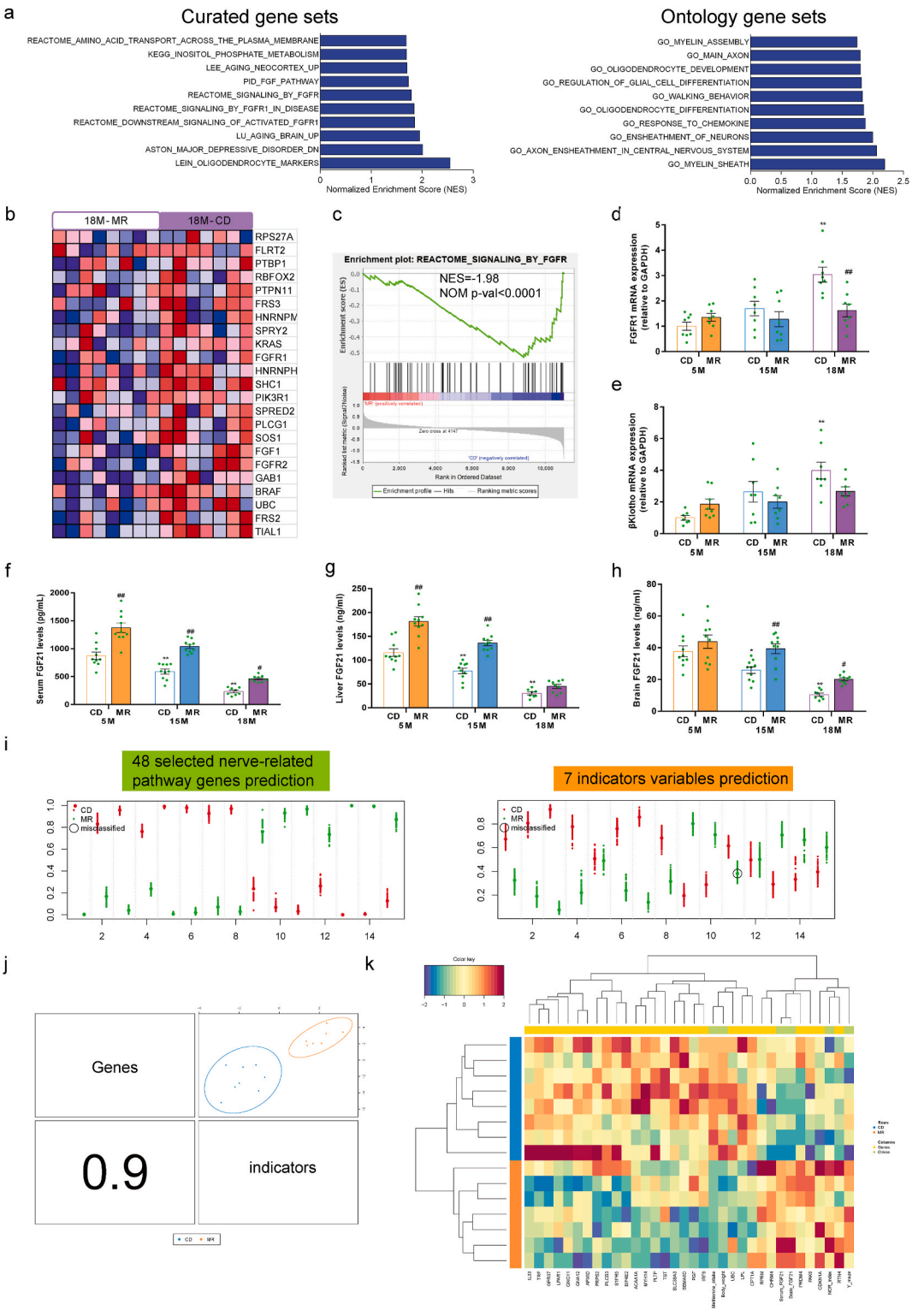

Fig. 3. Methionine restriction promoted serum FGF21 expression while it inhibited FGFR1 signaling in the hippocampus

(a) The bar graphs show normalized enrichment scores (NESs) of the gene set enrichment analysis (GSEA) on the curated gene sets and ontology gene sets for the RNA-seq analyses; **(b–c)** GSEA plot depicting the enrichment of downregulated genes involved in FGFR signaling in the 18M-MR group (NES = −1.98, NOR $p <$ 0.0001); **(d)** Expression of *Fgfr1* mRNA in the hippocampus was detected using RT-qPCR; **(e)** *β-klotho* mRNA expression in the hippocampus. FGF21 level in the **(f)** serum, **(g)** liver, and **(h)** brain. Data show mean ± SEM. *$p < 0.05$, **$p < 0.01$ compared to the CD group, Significant differences between mean values were determined using two-way ANOVA with Tukey's multiple comparison test. **(i)** The performance of predictive models for gene sets and signatures of characteristic indicators of MR status; **(j)** The model performance of DIABLO integrative modeling in relation to MR; **(k)** A clustered image map (Euclidean distance, complete linkage) of signatures. (For interpretation of the references to color in this figure legend, the reader is referred to the Web version of this article.)

serum, liver, and brain. MR significantly activated FGF21 levels in mice of all ages (two-way ANOVA with Tukey's test, $p < 0.01$; Fig. 3f–h).

The correlation between mouse performance, MR altered genes, and MR-mediated FGF21 activation was evaluated by integrated analyses using the Data Integration Analysis for Biomarker Discovery using a Latent Component method for OMICs (DIABLO), a multivariate dimension reduction discriminant analysis method designed to identify biologically relevant and highly correlated signatures from various OMICs techniques [37]. Behavioral performance, Met intake, and FGF21 content were selected as characteristic indicators and nervous system related genes as hub genes. First, we evaluated whether the MR-altered hub genes and characteristic indicators could predict the MR status of mice in a multivariate manner [38]. Predictive modeling was conducted using a partial least square discriminant analysis incorporated into a repeated double cross-validation framework (rdCV-PLSDA), which effectively minimized the risk of statistical overfitting [39]. We obtained 80 optimal separation genes from the 348 enriched genes and then selected 48 genes related to neural function based on literature regarding follow-up integrated analysis (Supplementary Fig. 4A). A significant separation between 18-month-old-CD and 18-month-old-MR mice was observed (Fig. 3i). Integrative modeling was then performed on the RNA-seq and characteristic indicator signatures, and one latent component comprising 7–8 key predictors from each data set was identified, contributing to a significant separation between the

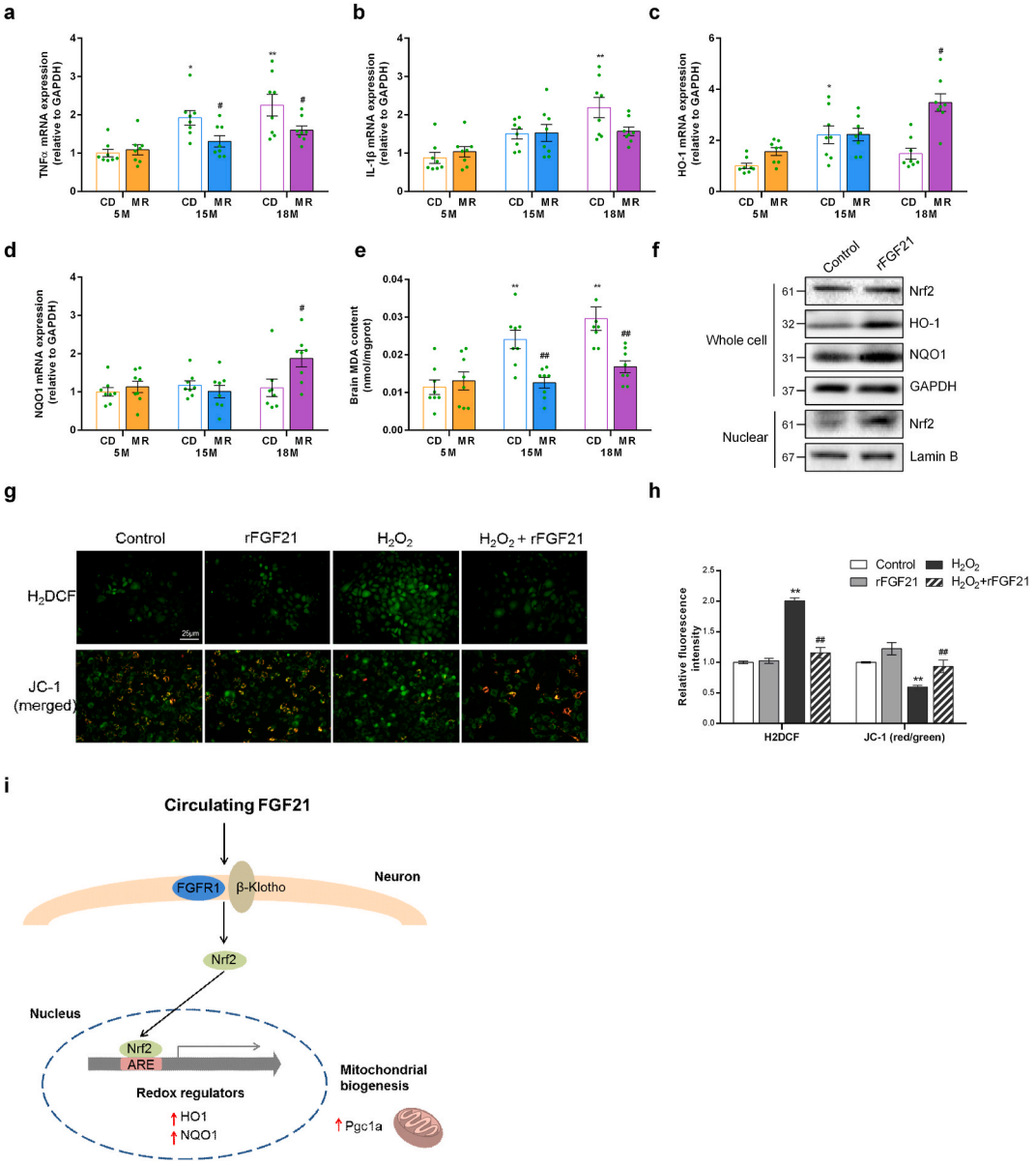

Fig. 4. Upregulation of Nrf2 was involved in FGF21-mediated MR protection against age-related neuroinflammation and oxidative stress
(a, b) *Tnfα* and *Il1β* mRNA expression in mice hippocampi; **(c, d)** *Ho1* and *Nqo1* mRNA expression in mice hippocampi; **(e)** MDA level in mouse brain. SH-SY5Y cells were treated with rFGF21 (100 μM) for 24 h. **(f)** Western blots of Nrf2 signaling pathway proteins. SH-SY5Y cells were treated with H_2O_2 (100 μM) for 24 h with or without treatment with rFGF21 (100 μM) for 24 h. Intracellular redox status was determined by dyeing with H_2DCFDA, and mitochondrial dysfunction was detected by staining with JC-1. **(g)** Representative images of H_2DCFDA and JC-1 staining; **(h)** Fluorescence was observed using an inverted fluorescence microscope. Data show mean ± SEM. $^*p < 0.05$, $^{**}p < 0.01$ compared to the control group. Significant differences between mean values were determined using two-way ANOVA with Tukey's multiple comparison test. **(i)** The proposed model for regulation of circulating FGF21-FGFR1/β-klotho-mediated activation of Nrf2 pathway. MR-mediated FGF21 promotes nuclear translocation of Nrf2, leading to improved neuroinflammation, oxidative stress, and mitochondrial biogenesis. The FGF21-Nrf2 axis may represent a novel target for treating age-related cognitive decline.

18-month-old-CD and 18-month-old-MR groups (Fig. 3g, Supplementary Fig. 4C). The key predictors were also highly correlated (Fig. 3k, Supplementary Fig. 4B).

3.4. FGF21 alleviates neuroinflammation and oxidative stress

We have shown previously that the effect of MR on cognitive function was associated with hippocampal neuron function (Fig. 2). Inflammation and oxidative homeostasis are closely related to neuronal cell function and cognitive functions [40]. The expression of inflammatory cytokines in the mouse hippocampus was determined using qPCR; results showed that the mRNA levels of *Tnfα* and *Il1β* increased significantly in the 18 month-old group. MR reduced the elevation of inflammatory factors (two-way ANOVA with Tukey's test, $p < 0.05$; Fig. 4a and b). Inflammatory responses often occur in conjunction with oxidative stress, and in our previous studies on aging mice, the levels of inflammatory factors and oxidative markers were found to increase simultaneously [31,32]. The Nrf2-derived antioxidant defense system, which leads to the transcriptional activation of HO1, NQO1, SOD2, and several antioxidant genes, is also present in nerve cells [41]. MR significantly increased the mRNA levels of *Ho1* and *Nqo1* in the hippocampi of 18-month-old mice (two-way ANOVA with Tukey's test, $p < 0.05$; Fig. 4c and d). MR also reduced malondialdehyde (MDA) levels, a lipid peroxidation product and marker of oxidative damage [42], in the cortex of aged mice (Fig. 4e). These results suggested that MR decreased neuroinflammation and oxidative stress in the hippocampi of aged mice.

In previous studies, FGF21 expression was significantly activated by MR and FGF21 possessed anti-inflammatory and antioxidant properties [43,44]. To further investigate whether FGF21 can activate antioxidant-signaling pathways in neurocytes, we treated SH-SY5Y cells with 100 nM rFGF21 and assessed the antioxidant enzyme levels. We observed that rFGF21 increased the expression of total Nrf2, HO1, and NQO1. rFGF21 increased the nuclear level of Nrf2, thus showing that rFGF21 promoted the nuclear translocation of Nrf2 (Fig. 4f). To determine whether or not the antioxidant enzymes activated by rFGF21 can improve oxidative stress, SH-SY5Y cells were pretreated with 100 μM H_2O_2, followed by treatment with 100 nM rFGF21. Using H_2DCFDA staining, reactive oxygen species (ROS) fluorescence was observed to increase after the H_2O_2 treatment of SH-SY5Y cells; however, rFGF21 treatment reduced fluorescence values (Fig. 4g). Mitochondrial membrane potential, evaluated by JC-1 staining, revealed that rFGF21 treatment alleviated oxidative stress (Fig. 4g). The quantitative analysis is shown in Fig. 4h. These results suggest that FGF21 might be a molecular target for MR to perform its neuroprotective functions (Fig. 4i).

3.5. FGF21 is required for the beneficial effects of MR

FGF21 was shown to improve HFD-induced cognitive impairments

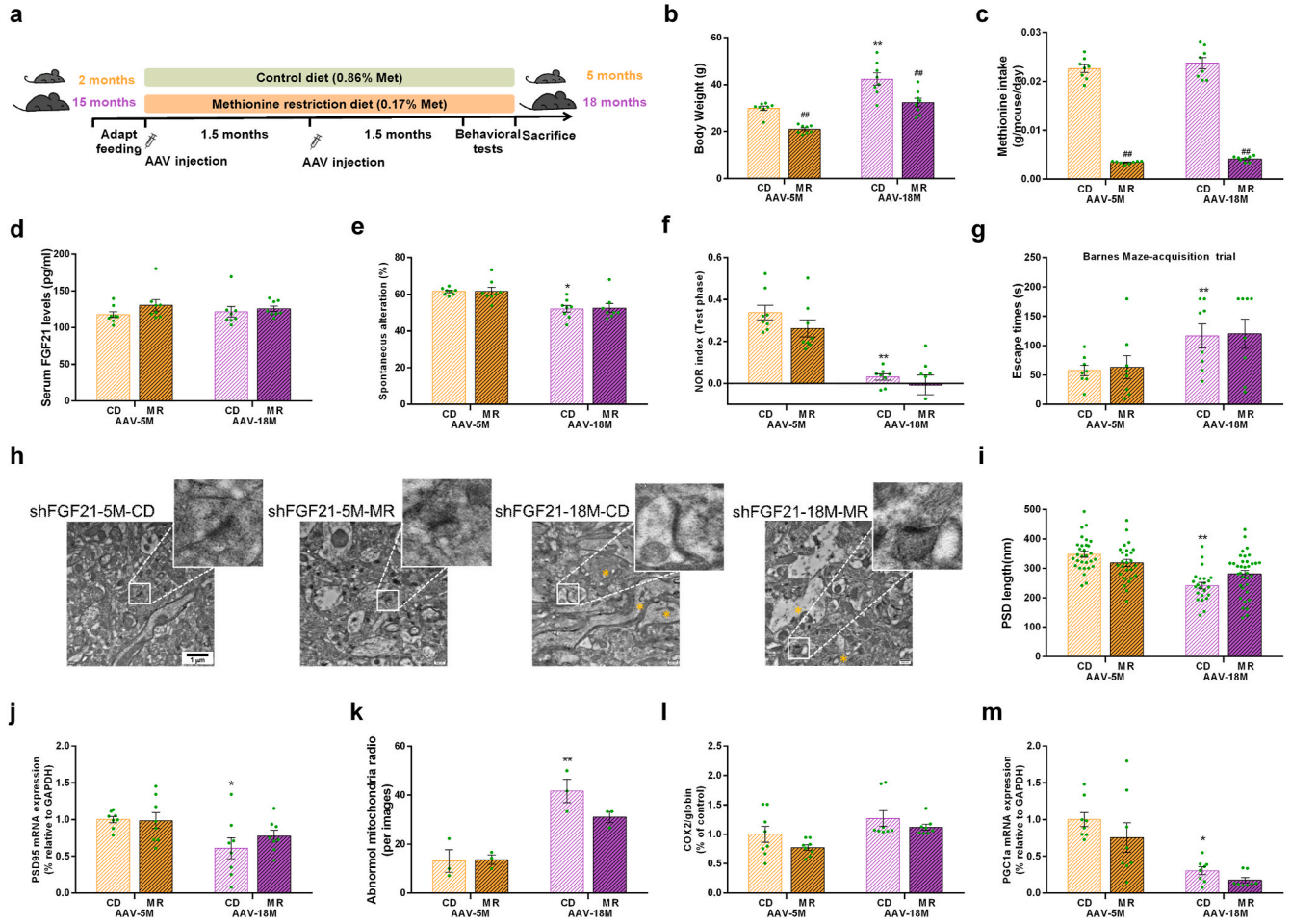

Fig. 5. FGF21 was required for MR-mediated improvement of cognitive impairment in aged mice.
(a) Schedule of animal treatments and behavior tests (n = 8 mice per group); **(b)** Bodyweight; **(c)** Methionine intake; **(d)** Serum FGF21 level. **(e)** Spontaneous alteration; **(f)** NOR index (new object); **(g)** Escape latency (Barnes maze test); **(h)** Representative images showing the ultrastructure of the synapse. The yellow asterisks indicate the abnormal mitochondria; **(i)** The length of PSD (n = 3 slices per group); **(j)** *Psd95* mRNA expression detected using RT-qPCR; **(k)** Abnormal mitochondria ratio; **(l)** Mitochondrial DNA levels in brain tissue; **(m)** *Pgc1α* mRNA expression in the hippocampus. Data show mean ± SEM. $*p < 0.05$, $**p < 0.01$ compared to the CD group. Significant differences between mean values were determined using two-way ANOVA with Tukey's multiple comparison test.

[26,45]; however, whether the neuroprotective function of MR requires FGF21 activation remains unclear. The crucial role of FGF21 in ameliorating age-related cognitive deficits was investigated by knocking down *Fgf21* in aged mice. Adeno-associated virus (AAV)-shFGF21 was synthesized for knocking down *Fgf21* in aged mice and a AAV loaded a scramble shRNA was used as a negative control. The *in vivo* silencing effects of AAV-shFGF21 were evaluated first (Supplementary Fig. 5 A-C). The results showed that AAV-shFGF21 treatment reduced serum, liver, and brain FGF21 levels in aged mice effectively; this inhibition was maintained for at least three weeks (Student's t-test, $p < 0.01$; Supplementary Fig. 5 D-F). Representative immunohistochemical images of the liver showed that AAV-shFGF21-mediated *Fgf21* silencing was sufficient. In addition, abnormal fat accumulation was observed in AAV-shFGF21-treated mice liver (Supplementary Fig. 5G).

Both 5- and 18-month-old mice were injected with AAV-shFGF21 via the tail vein, followed by a CD or MR interventions (Fig. 5a). In the AAV-5- and AAV-18 month-old groups, MR reduced the Met intake and body weight (ANOVA with Tukey's test, $p < 0.01$; Fig. 5b and c). The improved effect of MR on FGF21 expression was abolished by AAV treated in 18 month-old mice (Fig. 5d). Unexpectedly, MR still improved the age-related accumulation of adipocytes in the liver of aged mice with *Fgf21* knockdown (Supplementary Fig. 7).

Cognitive improvement, assessed using previous behavioral tests associated with MR, was partially abolished by *Fgf21* knockdown. Performance in the open field test was similar to that observed without AAV injection (Supplementary Fig. 6A–C). In particular, the improvement in spontaneous alteration (Y-maze), NOR index (NOR testing phase), and escape times (Barnes maze probe trial) were abolished by *Fgf21* knockdown (Fig. 5e–g, Supplementary Fig. 6D,E,G and H). In addition, AAV injection did not affect the morphology of neurons in the hippocampi of mice, although MR improved the shrinkage of neuronal nuclei (Supplementary Fig. 7). Analysis of PSD revealed that *Fgf21* knockdown reduced the length and width of PSD, which were elevated in 18-month-old-MR mice (Fig. 5h and i). The mRNA level of *Psd95* was also reduced in MR aged mice with *Fgf21* knockdown (Fig. 5j). Abnormal mitochondrial ratio, *Cox2*/globin ratio, and *Pgc1α* mRNA expression, upregulated in the 18-month-old-MR mice, were abrogated by *Fgf21* knockdown (Fig. 6k-m). The effects of MR on the oxidative stress and

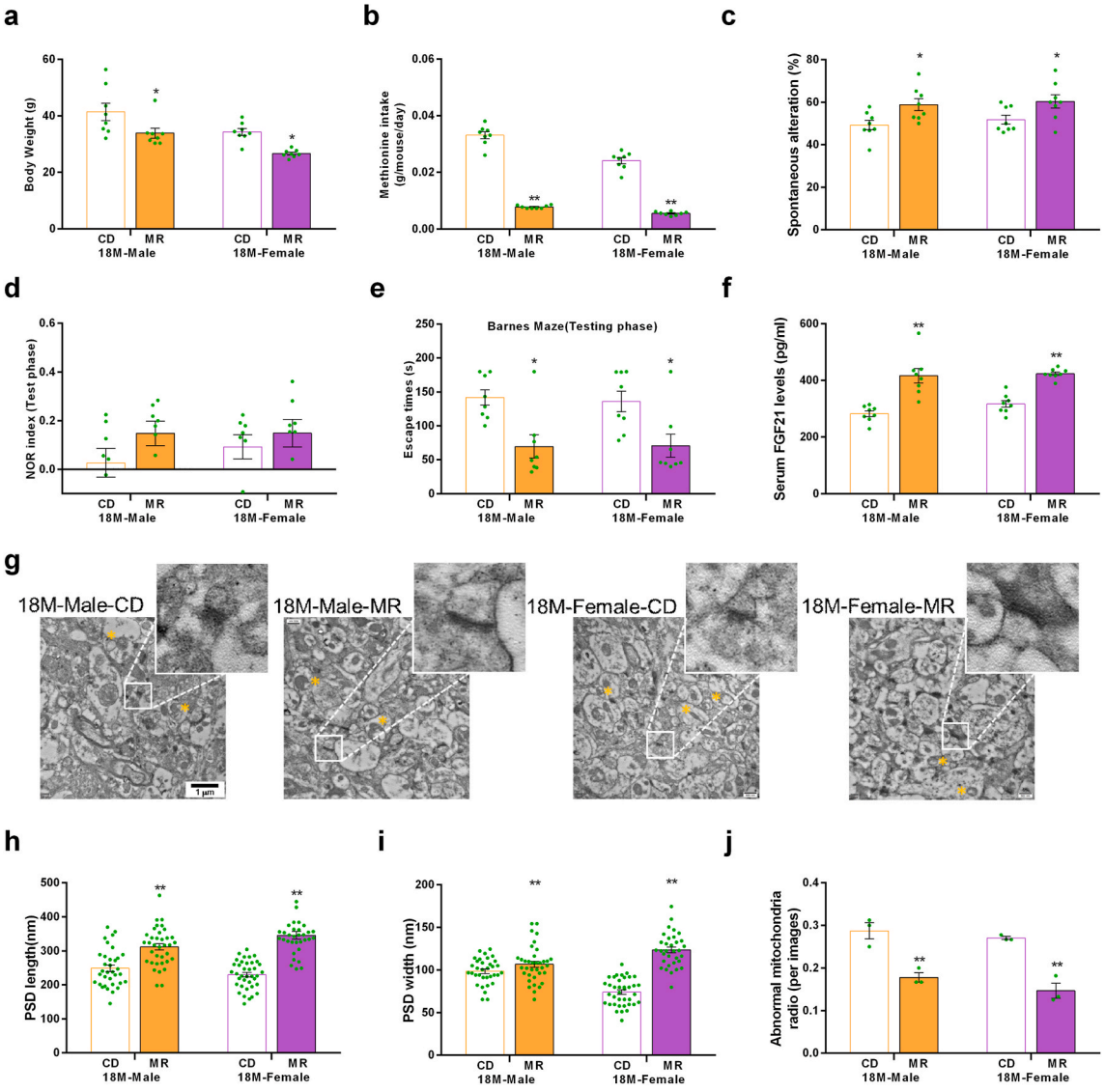

Fig. 6. MR improved the cognitive impairments and synaptic ultrastructure in aged male and female mice.
(a) Bodyweight (n = 8 mice per group); **(b)** Methionine intake; **(c)** Spontaneous alteration; **(d)** NOR index (new object); **(e)** Escape latency (Barnes maze test); **(f)** Serum FGF21 level; **(g)** Representative images showing the ultrastructure of the synapse. The yellow asterisks indicate the abnormal mitochondria; **(h, i)** The length and width of PSD (n = 3 slices per group); **(j)** Abnormal mitochondria ratio. Data show mean ± SEM. *$p < 0.05$, **$p < 0.01$ compared to the CD group. Significant differences between mean values were determined using two-way ANOVA with Tukey's multiple comparison test.

inflammation were partly abolished by FGF21 knockdown (Supplementary Fig. 6I–M). Collectively, these results indicate that FGF21 is required for the protective effects of MR on cognitive function.

Our previous studies were performed on male C57BL/6 J mice, which could limit the applicability of our findings, as female mice are known to respond differently to dietary challenges [46,47]. Hence, we repeated the dietary intervention on 15-month-old male and female mice. Body weight of aged male and female mice decreased under low Met intake (Fig. 6a and b). Serum FGF21 levels were high in aged mice subjected to MR intervention, irrespective of sex (Fig. 6f). The role of sex in MR-mediated changes in cognitive function was assessed by the behavioral paradigms mentioned above in terms of locomotor activity, working memory, short-term memory, and spatial memory. MR improved the performance of aged female mice in terms of spontaneous alteration (Y-maze), NOR index (NOR testing phase), and escape times (Barnes maze probe trial test), similar to aged male mice (Fig. 6c–e, Supplementary Fig. 8). Thus, it may be surmised that the effect of MR on the cognitive function of mice did not vary with sex. Synaptic structure in the hippocampi of mice also indicated that MR improved the synapse length and width of male and female aged mice (ANOVA with Tukey's test, $p < 0.01$; Fig. 6g–i). Mitochondrial morphology showed a similar response, with a lower number of abnormal mitochondria in both sexes (ANOVA with Tukey's test, $p < 0.01$; Fig. 6j).

4. Discussion

Previous studies have shown that MR extends lifespan in multiple organisms [48]. However, whether MR can alleviate age-related cognitive deficits is not known, and the underlying mechanism remains unclear. Our group and another independent group previously reported that MR improved cognitive functions in HFD-induced obese mice [15,16]. In this study, we demonstrated for the first time that a 3-month MR intervention alleviated age-related cognitive impairment, which depended on FGF21, a critical nutritional response mediated by MR, using comprehensive approaches on aged mice synaptic structure, mitochondrial biogenesis, and the Nrf2 signaling.

Aged mice showed cognitive decline in terms of loss of working-, short-term-, and spatial memory [31,32,49]. In particular, the neurological decline in aged mice is reflected in neuronal and synaptic structural damage in the hippocampus [31,32,49]. The RNA-seq data suggested that the neural processes-related pathways in the Kyoto Encyclopedia of Genes and Genomes (KEGG), including Alzheimer's disease, neurotrophin signaling pathway, and neuroactive ligand-receptor interaction, in the hippocampi of aged mice were altered by MR intervention (Supplementary Data 4 and 5). Brain mitochondria in young mice showed intact and parallel cristae, whereas those in aged mice exhibited vacuole cavitation, shrinkage, and reduction of mitochondrial cristae. Our previous data showed that MR improved cognitive decline in aged mice. Importantly, the correlation between behavioral performance, MR altered genes, and MR-mediated FGF21 activation observed in integrated analysis, suggest a pronounced contribution of FGF21 on MR improving age-related cognitive decline. The activation of MR on FGF21 expression is widely reported in previous studies [50–52]. MR was shown to increase *Fgf21* mRNA and protein levels in the serum and liver in both young and aged mice [51,52]. In the case of dietary MR, the hepatocytes sense the methionine insufficient and respond by activating the transcriptional programs of the cytoprotective, integrated stress response. General control nondepressible 2 (GCN2), an amino acid sensor, activates the phosphorylation of the eukaryotic initiation factor-2α (eIF-2α), which further activates activating the transcription factor 4 (ATF4) constituting the trophic response [52]. ATF4 binds to the responsive elements within the FGF21 promoter, leading to increased production of FGF21 [53].

Therefore, FGF21 circulation is maintained at high levels, including in the central nervous system. Previous studies showed that the activation of MR on circulating FGF21 decreased with mouse age [51]. However, we found that the FGF21 levels in the serum and liver were still significantly high in 18-month-old mice fed under MR for three months. In particular, the FGF21 content in the brain increased significantly (Fig. 3). In methionine-restricted obese mice, MR functioned in an FGF21-dependent and independent manner. MR regulated energy metabolism of adipose tissue by activating FGF21 signals in the brain [19]. However, MR decreased inflammatory responses of adipose tissue in an FGF21-independent manner [54]. In the current study, we focused on FGF21 as a neuroprotective factor of MR for two reasons: Firstly, it has been reported that hippocampal *Fgfr1* mRNA increased in major depression, schizophrenia, and bipolar disorder patients [55]. GSEA analysis of hippocampal RNA-seq data and PCR in this study showed that the hippocampal FGFR1 signal increased abnormally with aging. FGFR1 is indispensable for FGF21 function [56]. Secondly, in addition to its metabolic function, FGF21 also performs neuroprotective functions. FGF21 attenuates HFD-induced cognitive impairment via metabolic regulation and anti-inflammatory responses in obese mice [26]. FGF21 improves cognition by restoring synaptic plasticity, dendritic spine density, cerebral mitochondrial function, and cell apoptosis in obese insulin-resistant male rats [25]. We observed that the cognitive and neuroprotective functions of MR were lost after using AAV-shFGF21 to knockdown *Fgf21* expression. Notably, *Fgfr1* mRNA was decreased by MR treatment. It has been demonstrated that the FGFR1 mRNA levels were compensative up-regulated by diabetes-driven decreasing of plasma FGF21 in mice heart [57], which could be partly explained by the compensatory increase induced by age-related FGF21 insufficient. However, the relationship between FGFR1 deficiency and cognitive function is still unclear at the current stage. The effects of absence of FGFR1 on cognitive function should be investigated in the future research.

Reports on the mechanism underlying the neuroprotective function of FGF21 are limited. However, the mechanism via which FGF21 increases metabolism is known and is related to the activation of mitochondrial function and increase in mitochondrial biogenesis [27,58]. This is consistent with the results showing that MR improved mitochondrial morphology in the hippocampus and enhanced the expression of mitochondrial synthesis-related genes. Additionally, FGF21 can activate Nrf2 signaling via the FGFR/β-klotho receptor [45]. Our *in vitro* data showed that FGF21 treatment activated the Nrf2 signaling in SH-SY5Y cells and attenuated the oxidative damage induced by H_2O_2. This is consistent with the results showing that MR ameliorated hippocampal inflammation and enhanced the mRNA levels of the antioxidant enzymes *Ho-1* and *Nqo1 in vivo*. However, low-dose FGF21 reduced the inflammatory response in adipose tissue slightly. In this study, FGF21 reduced the expression of inflammatory factors in the hippocampus. As FGF21 is a major endogenous nutritional factor, its systemic administration cannot strictly be correlated with the neuroprotective function of FGF21.

The metabolic response to MR was reported to differ between males and females, although these studies were performed in young mice. Therefore, to extend the applicability of MR to protection against age-induced cognitive function, we repeated the experiments using 15-month-old male and female mice. Contrary to our expectations, FGF21 activation was not affected by sex. The mechanism underlying the difference in MR interventions between males and females were reported on obese mouse models [59,60]. The difference was mainly reflected in the metabolic response of male mice and the increase in FGF21-induced energy consumption, whereas the metabolic response of female mice was related to the reduction in energy intake. Nevertheless, the final weight reduction was due to MR, which is also consistent with our results. More relevant, MR activates the FGF21 expression in the liver and serum of both male and female mice. This supports the previous conclusion that MR improves the cognitive function of aging mice via FGF21. Based on the current results, it would be valuable to assess the effectiveness of MR on mouse models of Alzheimer's disease, which is associated with cognitive impairment.

It may be concluded that MR attenuates the cognitive decline caused by aging. The nutritional response signal, FGF21, is required for MR-mediated protection of neurological function and upregulation of hippocampal mitochondrial biogenesis. These results suggest that dietary restriction or specific essential amino acid restriction may be designed as nutritional interventions to prevent age-related cognitive disorders.

Author contributions

B.R., L.W., X.J. and Y.L. performed the experiments and analyzed the data, Z.L. and X.L. designed the study, Z.L., E.C., F.Y., R.L., X.D. and Z.L. wrote the paper, B.R., L.W., X.J. and L.S. prepared the figures. All authors discussed the results and commented on the paper.

Funding

This work was financially supported by the National Natural Science Foundation of China (81871118) and Innovative Talent Promotion Program-Technology Innovation Team (2019TD-006). Dr. Zhigang Liu is also funded by the Tang Cornell-China Scholars Program from Cornell University in the U.S. and the Alexander von Humboldt-Stiftung in Germany.

Declaration of competing interest

All authors declare that there are no conflicts of interest.

Appendix A. Supplementary data

Supplementary data to this article can be found online at https://doi.org/10.1016/j.redox.2021.101940.

References

[1] W. H. Organization, World Report on Ageing and Health, 2015.
[2] W. H. Organization, Global Strategy and Action Plan on Ageing and Health, 2017.
[3] U. Lindenberger, Human cognitive aging: corriger la fortune? Science 346 (2014) 572–578.
[4] I.J. Deary, J. Corley, A.J. Gow, S.E. Harris, L.M. Houlihan, R.E. Marioni, L. Penke, S.B. Rafnsson, J.M. Starr, Age-associated cognitive decline, Br. Med. Bull. 92 (2009) 135–152.
[5] L. Bordone, L. Guarente, Calorie restriction, SIRT1 and metabolism: understanding longevity, Nat. Rev. Mol. Cell Biol. 6 (2005) 298–305.
[6] X. Qiu, K. Brown, M.D. Hirschey, E. Verdin, D. Chen, Calorie restriction reduces oxidative stress by SIRT3-mediated SOD2 activation, Cell Metabol. 12 (2010) 662–667.
[7] L.M. Redman, S.R. Smith, J.H. Burton, C.K. Martin, D. Il'yasova, E. Ravussin, Metabolic slowing and reduced oxidative damage with sustained caloric restriction support the rate of living and oxidative damage theories of aging, Cell Metabol. 27 (2018) 805–815, e804.
[8] T. Laeger, D.C. Albarado, S.J. Burke, L. Trosclair, J.W. Hedgepeth, H.-R. Berthoud, T.W. Gettys, J.J. Collier, H. Münzberg, C.D. Morrison, Metabolic responses to dietary protein restriction require an increase in FGF21 that is delayed by the absence of GCN2, Cell Rep. 16 (2016) 707–716.
[9] H.S. Shim, V.D. Longo, A protein restriction-dependent sulfur code for longevity, Cell 160 (2015) 15–17.
[10] C. Ruckenstuhl, C. Netzberger, I. Entfellner, D. Carmona-Gutierrez, T. Kickenweiz, S. Stekovic, C. Gleixner, C. Schmid, L. Klug, A.G. Sorgo, Lifespan extension by methionine restriction requires autophagy-dependent vacuolar acidification, PLoS Genet. 10 (2014) e1004347.
[11] B.C. Lee, A. Kaya, S. Ma, G. Kim, M.V. Gerashchenko, S.H. Yim, Z. Hu, L. G. Harshman, V.N. Gladyshev, Methionine restriction extends lifespan of Drosophila melanogaster under conditions of low amino-acid status, Nat. Commun. 5 (2014) 1–12.
[12] L. Sun, A.A. Sadighi Akha, R.A. Miller, J.M. Harper, Life-span extension in mice by preweaning food restriction and by methionine restriction in middle age, J. Gerontol. A Biol. Sci. Med. Sci. 64 (2009) 711–722.
[13] A. Naudi, P. Caro, M. Jove, J. Gomez, J. Boada, V. Ayala, M. Portero-Otin, G. Barja, R. Pamplona, Methionine restriction decreases endogenous oxidative molecular damage and increases mitochondrial biogenesis and uncoupling protein 4 in rat brain, Rejuvenation Res. 10 (2007) 473–484.
[14] M. Jové, V.r. Ayala, O. Ramirez-Nunez, A. Naudi, R. Cabré, C.M. Spickett, M. Portero-Otín, R. Pamplona, Specific lipidome signatures in central nervous system from methionine-restricted mice, J. Proteome Res. 12 (2013) 2679–2689.
[15] Y. Xu, Y. Yang, J. Sun, Y. Zhang, T. Luo, B. Li, Y. Jiang, Y. Shi, G. Le, Dietary methionine restriction ameliorates the impairment of learning and memory function induced by obesity in mice, Food Funct. 10 (2019) 1411–1425.
[16] L. Wang, B. Ren, Y. Hui, C. Chu, Z. Zhao, Y. Zhang, B. Zhao, R. Shi, J. Ren, X. Dai, Methionine restriction regulates cognitive function in high-fat diet-fed mice: roles of diurnal rhythms of SCFAs producing-and inflammation-related microbes, Mol. Nutr. Food Res. 64 (2020) 2000190.
[17] K.R. Markan, M.C. Naber, M.K. Ameka, M.D. Anderegg, D.J. Mangelsdorf, S. A. Kliewer, M. Mohammadi, M.J. Potthoff, Circulating FGF21 is liver derived and enhances glucose uptake during refeeding and overfeeding, Diabetes 63 (2014) 4057–4063.
[18] D. Wanders, L.A. Forney, K.P. Stone, D.H. Burk, A. Pierse, T.W. Gettys, FGF21 mediates the thermogenic and insulin-sensitizing effects of dietary methionine restriction but not its effects on hepatic lipid metabolism, Diabetes 66 (2017) 858–867.
[19] L.A. Forney, H. Fang, L.C. Sims, K.P. Stone, L.Y. Vincik, A.M. Vick, A.N. Gibson, D. H. Burk, T.W. Gettys, Dietary methionine restriction signals to the brain through fibroblast growth factor 21 to regulate energy balance and remodeling of adipose tissue, Obesity 28 (2020) 1912–1921.
[20] H. Land, C. West, J. Stern, T. Gettys, D. Wanders, P. Perez, K. Chiang, Mechanisms of action of methionine restriction and fibroblast growth factor 21 (FGF21), Curr. Dev. Nutr. 4 (2020), 1218–1218.
[21] A. Salminen, A. Kauppinen, K. Kaarniranta, FGF21 activates AMPK signaling: impact on metabolic regulation and the aging process, J. Mol. Med. 95 (2017) 123–131.
[22] Y. Yu, F. Bai, W. Wang, Y. Liu, Q. Yuan, S. Qu, T. Zhang, G. Tian, S. Li, D. Li, Fibroblast growth factor 21 protects mouse brain against D-galactose induced aging via suppression of oxidative stress response and advanced glycation end products formation, Pharmacol. Biochem. Behav. 133 (2015) 122–131.
[23] A.L. Bookout, M.H. De Groot, B.M. Owen, S. Lee, L. Gautron, H.L. Lawrence, X. Ding, J.K. Elmquist, J.S. Takahashi, D.J. Mangelsdorf, FGF21 regulates metabolism and circadian behavior by acting on the nervous system, Nat. Med. 19 (2013) 1147.
[24] M. Kuroda, R. Muramatsu, N. Maedera, Y. Koyama, M. Hamaguchi, H. Fujimura, M. Yoshida, M. Konishi, N. Itoh, H. Mochizuki, Peripherally derived FGF21 promotes remyelination in the central nervous system, J. Clin. Invest. 127 (2017) 3496–3509.
[25] P. Sa-nguanmoo, P. Tanajak, S. Kerdphoo, P. Satjaritanun, X. Wang, G. Liang, X. Li, C. Jiang, W. Pratchayasakul, N. Chattipakorn, FGF21 improves cognition by restored synaptic plasticity, dendritic spine density, brain mitochondrial function and cell apoptosis in obese-insulin resistant male rats, Horm, Beyond Behav. 85 (2016) 86–95.
[26] Q. Wang, J. Yuan, Z. Yu, L. Lin, Y. Jiang, Z. Cao, P. Zhuang, M.J. Whalen, B. Song, X.-J. Wang, FGF21 attenuates high-fat diet-induced cognitive impairment via metabolic regulation and anti-inflammation of obese mice, Mol. Neurobiol. 55 (2018) 4702–4717.
[27] J. Mäkelä, T.V. Tselykh, F. Maiorana, O. Eriksson, H.T. Do, G. Mudò, L. T. Korhonen, N. Belluardo, D. Lindholm, Fibroblast growth factor-21 enhances mitochondrial functions and increases the activity of PGC-1α in human dopaminergic neurons via Sirtuin-1, SpringerPlus 3 (2014) 2.
[28] Z. Liu, X. Dai, H. Zhang, R. Shi, Y. Hui, X. Jin, W. Zhang, L. Wang, Q. Wang, D. Wang, Gut microbiota mediates intermittent-fasting alleviation of diabetes-induced cognitive impairment, Nat. Commun. 11 (2020) 1–14.
[29] A. Subramanian, P. Tamayo, V.K. Mootha, S. Mukherjee, B.L. Ebert, M.A. Gillette, A. Paulovich, S.L. Pomeroy, T.R. Golub, E.S. Lander, Gene set enrichment analysis: a knowledge-based approach for interpreting genome-wide expression profiles, in: Proc. Natl. Acad. Sci. U.S.A., vol. 102, 2005, pp. 15545–15550.
[30] V.K. Mootha, C.M. Lindgren, K.-F. Eriksson, A. Subramanian, S. Sihag, J. Lehar, P. Puigserver, E. Carlsson, M. Ridderstråle, E. Laurila, PGC-1α-responsive genes involved in oxidative phosphorylation are coordinately downregulated in human diabetes, Nat. Genet. 34 (2003) 267–273.
[31] B. Ren, T. Yuan, X. Zhang, L. Wang, J. Pan, Y. Liu, B. Zhao, W. Zhao, Z. Liu, X. Liu, Protective effects of sesamol on systemic inflammation and cognitive impairment in aging mice, J. Agric. Food Chem. 68 (2020) 3099–3111.
[32] B. Zhao, H. Liu, J. Wang, P. Liu, X. Tan, B. Ren, Z. Liu, X. Liu, Lycopene supplementation attenuates oxidative stress, neuroinflammation, and cognitive impairment in aged CD-1 mice, J. Agric. Food Chem. 66 (2018) 3127–3136.
[33] C.V. Vorhees, M.T. Williams, Morris water maze: procedures for assessing spatial and related forms of learning and memory, Nat. Protoc. 1 (2006) 848.
[34] F. Harrison, A. Hosseini, M. McDonald, Endogenous anxiety and stress responses in water maze and Barnes maze spatial memory tasks, Behav. Brain Res. 198 (2009) 247–251.
[35] H. Eichenbaum, Hippocampus: cognitive processes and neural representations that underlie declarative memory, Neuron 44 (2004) 109–120.
[36] I. Ehrlich, R. Malinow, Postsynaptic density 95 controls AMPA receptor incorporation during long-term potentiation and experience-driven synaptic plasticity, J. Neurosci. 24 (2004) 916–927.
[37] F. Rohart, B. Gautier, A. Singh, K.-A. Lê Cao, mixOmics: an R package for 'omics feature selection and multiple data integration, PLoS Comput. Biol. 13 (2017) e1005752.
[38] S. Rowan, S. Jiang, T. Korem, J. Szymanski, M.-L. Chang, J. Szelog, C. Cassalman, K. Dasuri, C. McGuire, R. Nagai, Involvement of a gut–retina axis in protection against dietary glycemia-induced age-related macular degeneration, in: Proc. Natl. Acad. Sci. U.S.A., vol. 114, 2017, pp. E4472–E4481.
[39] L. Shi, J.A. Westerhuis, J. Rosén, R. Landberg, C. Brunius, Variable selection and validation in multivariate modelling, Bioinformatics 35 (2019) 972–980.

[40] M. Baierle, S.N. Nascimento, A.M. Moro, N. Brucker, F. Freitas, B. Gauer, J. Durgante, S. Bordignon, M. Zibetti, C.M. Trentini, Relationship between inflammation and oxidative stress and cognitive decline in the institutionalized elderly, Oxid. Med. Cell. Longevity 2015 (2015).
[41] T.T. Hoang, D.A. Johnson, R.T. Raines, J.A. Johnson, Angiogenin activates the astrocytic Nrf2/antioxidant-response element pathway and thereby protects murine neurons from oxidative stress, J. Biol. Chem. 294 (2019) 15095–15103.
[42] J. Greilberger, C. Koidl, M. Greilberger, M. Lamprecht, K. Schroecksnadel, F. Leblhuber, D. Fuchs, K. Oettl, Malondialdehyde, carbonyl proteins and albumin-disulphide as useful oxidative markers in mild cognitive impairment and Alzheimer's disease, Free Radic. Res. 42 (2008) 633–638.
[43] Y. Yu, J. He, S. Li, L. Song, X. Guo, W. Yao, D. Zou, X. Gao, Y. Liu, F. Bai, Fibroblast growth factor 21 (FGF21) inhibits macrophage-mediated inflammation by activating Nrf2 and suppressing the NF-κB signaling pathway, Int. Immunopharm. 38 (2016) 144–152.
[44] M.Á. Gómez-Sámano, M. Grajales-Gómez, J.M. Zuarth-Vázquez, M.F. Navarro-Flores, M. Martínez-Saavedra, Ó.A. Juárez-León, M.G. Morales-García, V. M. Enríquez-Estrada, F.J. Gómez-Pérez, D. Cuevas-Ramos, Fibroblast growth factor 21 and its novel association with oxidative stress, Redox Biol. 11 (2017) 335–341.
[45] Z. Yu, L. Lin, Y. Jiang, I. Chin, X. Wang, X. Li, E.H. Lo, X. Wang, Recombinant FGF21 protects against blood-brain barrier leakage through Nrf2 upregulation in type 2 diabetes mice, Mol. Neurobiol. 56 (2019) 2314–2327.
[46] R.A. Miller, D.E. Harrison, C.M. Astle, E. Fernandez, K. Flurkey, M. Han, M. A. Javors, X. Li, N.L. Nadon, J.F. Nelson, Rapamycin-mediated lifespan increase in mice is dose and sex dependent and metabolically distinct from dietary restriction, Aging Cell 13 (2014) 468–477.
[47] B. Martin, M. Pearson, L. Kebejian, E. Golden, A. Keselman, M. Bender, O. Carlson, J. Egan, B. Ladenheim, J.-L. Cadet, Sex-dependent metabolic, neuroendocrine, and cognitive responses to dietary energy restriction and excess, Endocrinology 148 (2007) 4318–4333.
[48] R.S. McIsaac, K.N. Lewis, P.A. Gibney, R. Buffenstein, From yeast to human: exploring the comparative biology of methionine restriction in extending eukaryotic life span, Ann. N. Y. Acad. Sci. 1363 (2016) 155–170.
[49] S.A. Villeda, K.E. Plambeck, J. Middeldorp, J.M. Castellano, K.I. Mosher, J. Luo, L. K. Smith, G. Bieri, K. Lin, D. Berdnik, Young blood reverses age-related impairments in cognitive function and synaptic plasticity in mice, Nat. Med. 20 (2014) 659–663.
[50] K.P. Stone, D. Wanders, M. Orgeron, C.C. Cortez, T.W. Gettys, Mechanisms of increased in vivo insulin sensitivity by dietary methionine restriction in mice, Diabetes 11 (2014) 3721–3733.
[51] E.K. Lees, E. Król, L. Grant, K. Shearer, C. Wyse, E. Moncur, A.S. Bykowska, N. Mody, T.W. Gettys, M. Delibegovic, Methionine restriction restores a younger metabolic phenotype in adult mice with alterations in fibroblast growth factor 21, Aging Cell 13 (2014) 817–827.
[52] D. Wanders, K.P. Stone, L.A. Forney, C.C. Cortez, K.N. Dille, J. Simon, M. Xu, E. C. Hotard, I.A. Nikonorova, A.P. Pettit, Role of GCN2-independent signaling through a noncanonical PERK/NRF2 pathway in the physiological responses to dietary methionine restriction, Diabetes 65 (2016) 1499–1510.
[53] A.L. De Sousa-Coelho, P.F. Marrero, D. Haro, Activating transcription factor 4-dependent induction of FGF21 during amino acid deprivation, Biochem. J. 443 (2012) 165–171.
[54] S. Sharma, T. Dixon, S. Jung, E.C. Graff, L.A. Forney, T.W. Gettys, D. Wanders, Dietary methionine restriction reduces inflammation independent of FGF21 action, Obesity 27 (2019) 1305–1313.
[55] F. Gaughran, J. Payne, P.M. Sedgwick, D. Cotter, M. Berry, Hippocampal FGF-2 and FGFR1 mRNA expression in major depression, schizophrenia and bipolar disorder, Brain Res, Bull. (Arch. Am. Art) 70 (2006) 221–227.
[56] T. Lan, D.A. Morgan, K. Rahmouni, J. Sonoda, X. Fu, S.C. Burgess, W.L. Holland, S. A. Kliewer, D.J. Mangelsdorf, FGF19, FGF21, and an FGFR1/β-Klotho-activating antibody act on the nervous system to regulate body weight and glycemia, Cell Metabol. 26 (2017) 709–718, e703.
[57] X. Yan, J. Chen, C. Zhang, S. Zhou, Z. Zhang, J. Chen, W. Feng, X. Li, Y. Tan, FGF21 deletion exacerbates diabetic cardiomyopathy by aggravating cardiac lipid accumulation, J. Cell Mol. Med. 19 (2015) 1557–1568.
[58] X.-M. Wang, H. Xiao, L.-L. Liu, D. Cheng, X.-J. Li, L.-Y. Si, FGF21 represses cerebrovascular aging via improving mitochondrial biogenesis and inhibiting p53 signaling pathway in an AMPK-dependent manner, Exp. Cell Res. 346 (2016) 147–156.
[59] L.A. Forney, K.P. Stone, A.N. Gibson, A.M. Vick, L.C. Sims, H. Fang, T.W. Gettys, Sexually dimorphic effects of dietary methionine restriction are dependent on age when the diet is introduced, Obesity 28 (2020) 581–589.
[60] K.A. Dyar, D. Lutter, A. Artati, N.J. Ceglia, Y. Liu, D. Armenta, M. Jastroch, S. Schneider, S. de Mateo, M. Cervantes, Atlas of circadian metabolism reveals system-wide coordination and communication between clocks, Cell 174 (2018) 1571–1585, e1511.